Crystal substructure and physical properties of the superconducting phase $Bi_4(Sr,Ca)_6Cu_4O_{16+x}$

J. M. Tarascon
Bellcore, 331 Newman Springs Road, Red Bank, New Jersey 07701

Y. Le Page
National Research Council of Canada, Ottawa, Canada

P. Barboux, B. G. Bagley, and L. H. Greene
Bellcore, 331 Newman Springs Road, Red Bank, New Jersey 07701

W. R. McKinnon
National Research Council of Canada, Ottawa, Canada

G. W. Hull, M. Giroud, and D. M. Hwang
Bellcore, 331 Newman Springs Road, Red Bank, New Jersey 07701
(Received 11 February 1988)

We have isolated a high-T_c phase in the Bi-Sr-Ca-Cu-O system of composition $Bi_4(Sr,Ca)_6Cu_4O_{16+x}$. The crystal substructure has a tetragonal unit cell ($a=3.817$ Å, $c=30.5$ Å) with similarities to both the oxygen-defect perovskites $YBa_2Cu_3O_{7-x}$ and the K_2NiF_4 structure of La_2CuO_4. The oxygen content, determined by titration and thermogravimetric analysis experiments, corresponds to a formal oxidation state Cu(2.15). Oxygen can be reversibly depleted in an argon ambient in an amount corresponding to the reduction of the Cu(III) into Cu(II). The compound has a metalliclike resistance above its T_c near 85 K. Processing this precursor compound by heating to temperatures near its melting point (885 °C) produces a sharp resistivity drop near 110 K that we show by ac susceptibility and Meissner effect is due to a superconducting transition.

INTRODUCTION

The discovery of Bednorz and Müller[1] of high-temperature superconductivity in the Ba-La-Cu-O system led to the subsequent discovery by Wu *et al.*[2] of high-temperature superconductivity in the Y-Ba-Cu-O system. A number of different high-temperature superconducting compounds have been prepared based on elemental substitutions in these two systems. In general, these oxide materials contain as cations Cu, a critical element for the occurrence of superconductivity, an alkaline earth, and a rare earth or yttrium. Recently, cuprate superconductors have been prepared[3–6] which contain Bi but no rare earth or yttrium. Maeda, Tanaka, Fukutomi, and Asano[5] report that the composition $BiSrCaCu_2O_x$ (we denote compositions by cation stoichiometry, here, 1:1:1:2) has a resistance T_c of about 105 K (but with a low-temperature "tail" that extends to about 80 K) and that the oxide must contain both Sr and Ca if it is to have a high T_c. We have isolated a high-T_c phase in the Bi-Sr-Ca-Cu-O system, determined its structure, measured some of its properties, and report here our results.[7]

SYNTHESIS

A number of compositions in the Bi-Sr-Ca-Cu-O system (including the 1:1:1:2 stoichiometry reported by Maeda *et al.*[5]) were prepared from a mixture of bismuth oxide, copper oxide, strontium carbonate, and calcium carbonate (each 99.999% pure). The samples were heated in oxygen for 12 h at temperatures ranging from 800 to 900 °C, ground, reannealed for 12 h more at 860 °C, and then cooled (in oxygen) to room temperature over a period of 2 h. The resulting materials were well-crystallized black powders with a few plateletlike crystals. On grinding, the morphology of these powders appears to be similar to those of layered materials, suggesting a two-dimensional character. For resistivity measurements, a part of each sample was pressed into a 1.3 cm diameter pellet, reannealed, and cut into rectangular bars. From our powder-diffraction measurements obtained with a Scintag diffractometer using Cu $K\alpha$ radiation, we conclude that the 1:1:1:2 composition is multiphase. The two superconducting transition temperatures observed at 85 and 110 K by resistivity measurements[5] could thus be due to two phases or the result of different processing treatments.

We determined from our powder-diffraction experiments that there is a single-phase compound formed at the composition $Bi_4Sr_3Ca_3Cu_4O_y$ (4:3:3:4). The range of reaction temperature at which the nominal composition 4:3:3:4 gives a single-phase material is very narrow (865 °C ± 10 °C). However, we find that by starting with the nominal composition 4:3:3:6 we can more easily obtain a material with the x-ray powder pattern of the 4:3:3:4

phase but with, of course, two extra peaks located at $2\theta = 35.45$ and 38.73 corresponding to CuO. Figure 1(a) shows the x-ray powder-diffraction pattern of a material of nominal composition 4:3:3:4 over the 2θ range from 5 to 65° with the h,k,l Miller indices noted above each peak. For this material all the Bragg diffraction peaks could be completely indexed on the basis of a tetragonal unit cell with $a = 3.818(5)$ Å, $c = 30.6$ Å, and $V = 447$ Å^3. We were able to prepare large (2.5 mm × 4 mm × 100 μm), well-oriented, polycrystalline composites for further investigation. These composites were prepared by using excess bismuth oxide which, at the sample preparation temperature close to the melting point of the 4:3:3:4 phase, acted as a flux. When a planar sample was prepared on a quartz slide, the platelet nature of the 4:3:3:4 compound produced a preferred orientation with the c axis normal to the sample surface. The x-ray powder diffraction from this oriented multicrystal composite is shown in Fig. 1(b). In this pattern only the 0,0,1 reflections appear from which a c axis of 15.3 Å was determined. However, to fit the x-ray powder pattern of this new phase, a doubling of the unit cell was required ($c = 30.6$ Å), and thus the 001 indexes with 1 even.

We also varied the strontium-calcium ratio in the $Bi_4Sr_{3+x}Ca_{3-x}Cu_6O_y$ composition series in steps of $\Delta x = 0.25$ from $x = -0.5$ to $x = 0.5$. Again we note that, for reasons which are not clear, it is easier to obtain the $Bi_4(Sr,Ca)_6Cu_4O_{16+x}$ phase when there is excess CuO present. For these compositions, with the exception of the Bragg peaks corresponding to the CuO impurity phase, the materials were single phase. We observe no detectable change in lattice parameter or in T_c (within ±2 K) between the various compositions. A solid solution appears to exist over the composition range $x < \pm 0.5$ but beyond $x = \pm 0.5$ the compound is definitely no longer single phase. We also point out that our attempts to prepare a phase of nominal composition 4:4:2:4 (4 strontiums and 2 calciums) resulted in a multiphase system independent of the thermal treatment, whereas a single-phase material is obtained with the nominal composition 4:3:3:4.

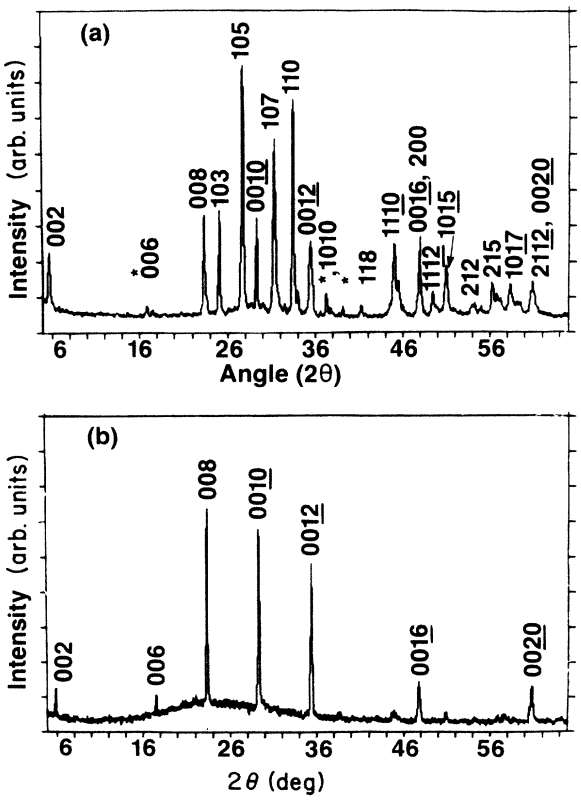

FIG. 1. X-ray powder diffraction pattern of the 4:3:3:4 material is shown over the 2θ range from 5 to 65°. The pattern for a polycrystalline powder is shown in (a) with the Miller indices noted above each peak. Shown in (b) is the pattern for highly c-oriented multicrystalline composite (sample C). Note that only the (001) reflections with 1 even are observed. Peaks with asterisks can be indexed in a unit cell of $a = 5.4$ and $c = 30.6$ Å.

CRYSTAL STRUCTURE

A superconducting powder was separated with a magnet making use of the Meissner effect in liquid nitrogen. A single crystal 16 × 70 × 120 μm was selected and mounted on a Picker diffractometer with graphite-monochromatized Cu $K\alpha$ radiation. The body-centered tetragonal cell derived from the interpretation of the powder pattern was confirmed. The cell parameters $a = 3.814$ Å and $c = 30.52$ Å obtained on this crystal are quite poor because the crystals are buckled due to their small thickness. Due to this buckling, the normal to the atomic planes changes direction with the point on the crystal. Consequently, the reciprocal lattice nodes are spread out on circular arcs parallel to [001] for $hk0$ reflections and on a spherical cap for 001 reflections. This angular spreading of about 1° ruled out the use of Mo radiation because of reflection overlap; therefore, we used the Cu radiation. Even with this longer x-ray wavelength reflection overlap was not completely eliminated, and also, part of the diffracted intensity did not reach the counter for large Bragg angles. In spite of these experimental difficulties, crude diffraction intensities could be measured. A survey of reflection intensities symmetry-related in Laue group $4/mmm$ but not in Laue group $4/m$ indicated Laue group $4/mmm$. The reflection profiles were displayed on a screen for comparison. Intensity measurements up to 120° Bragg angle followed by averaging of the symmetry-related intensities after absorption correction by Gaussian integration gave 143 unique reflections, 111 of which were observed.

Although the tetragonal diffraction aspect I--- combined with Laue class $4/mmm$ allows the space group $I422$, $I\bar{4}mm$, $I\bar{4}m2$, $I42m$, and $I4/mmm$, the very short a and b repeats force the fractional coordinates for the metal atoms to be 0 and $\frac{1}{2}$ for an ordered tetragonal structure in all these space groups. As the diffraction intensities do not contain a class of reflections so weak that it could be due to oxygen only, it follows that the metal contribution, which dominates the diffraction intensities for all classes of reflections, can be phased in space groups $I4mm$ or $I4/mmm$. The reflections being phased by the metals, the oxygens should be visible on difference-Fourier maps and lower symmetry should be indicated by split peaks on the

difference maps or by fractional refined occupancies. The space group *I4/mmm*, which is centrosymmetric, is more likely for a high-temperature oxide.

The Patterson map indicated that the trial Bi positions were either $(0,0,\frac{3}{10})$ or $(0,0,\frac{4}{10})$. A succession of least-squares refinement cycles followed by difference-Fourier maps confirmed the position at $(0,0,\frac{3}{10})$ and gave the structure description in Table I. The residuals are $R_f=0.16$, $R_{wf}=0.10$ on 111 observed reflections refined with 8 parameters. Isotropic thermal parameters were fixed at $B=3.6$ Å^2 for all atoms and not refined. Complete ordering of Ca and Sr as well as full occupancy of the sites in the slabs was assumed at this point. The residuals are very poor, due to the data collection difficulties and to the very large absorption correction, which is critically dependent on the thickness of the sample, which was measured with a microscope. It should be remembered that most known structure types have been obtained with eye-estimated intensities of similar quality. Our confidence in this semiquantitative model comes from the fact that it is made of known building blocks also seen in other superconductors and that it obeys the principle of local electroneutrality. The bond distances are given in Table II. They are quite crude, especially those which are parallel to *c*.

The structure has similarities with both $YBa_2Cu_3O_7$ (1:2:3 composition) and La_2CuO_4. In the present structure, Ca in a cube at the cell center has the same polyhedral environment as Y in $YBa_2Cu_3O_7$, sharing edges with eight CuO_5 pyramids and faces with two Sr polyhedra. Sr plays the same role as Ba in $YBa_2Cu_3O_7$, but it is ninefold-coordinated as La in La_2CuO_4, leaving large pyramidal sites occupied by Bi (Fig. 2).

TABLE I. Crystal data for the tetragonal substructure in $Bi_2Sr_2CaCu_2O_{8.13}$. The space group is tetragonal: *I4/mmm* with $a=3.814(3)$, $c=30.52(3)$ with two formula units in the cell. The incommensurate superstructure along [110] leads to a larger cell and lower crystal system. 143 unique reflection intensities were measured with Cu $K\alpha$ radiation up to 120° Bragg angle using a sample measuring $16\times70\times120$ μm and then corrected for absorption by Gaussian integration. The final residuals are $R_f=0.16$ and $R_{wf}=0.10$ using counting statistics weights on 111 reflections larger than 2.5σ and considered to be observed. The isotropic thermal motion was fixed at $B=3.6$ Å^2 and 8 parameters were used in the refinement. The final positional parameters are shown below. Estimated standard deviations refer to the last digit printed.

Atom	Wyckoff	x	y	z	B	Site occupancy
Ca	2*a*	0	0	0	3.6	
Sr	4*e*	0	0	0.1097(5)	3.6	
Bi	4*e*	0	0	0.3022(3)	3.6	0.87
Bi'	4*e*	0	0	0.2681(18)	3.6	0.13
Cu	4*e*	0	0	0.4456(9)	3.6	
O(1)	8*g*	$\frac{1}{2}$	0	0.446(3)	3.6	
O(2)	4*e*	0	0	0.375(4)	3.6	
O(3)	4*e*	0	0	0.205(4)	3.6	
O(4)	4*d*	$\frac{1}{2}$	0	$\frac{1}{4}$	3.6	0.065

TABLE II. Important metal-oxygen distances. Bond distance for Bi–O(3) [2.97(11)×1] is distance from slab to slab.

Structure	Bond distance
Ca–O(1)	2.52(5)×8
Sr–O(1)	2.56(5)×4
Sr–O(2)	2.74(2)×4
Sr–O(3)	2.91(11)×1
Bi–O(2)	2.22(7)×1
Bi–O(3)	2.71(1)×4
Bi–O(3)	2.97(11)×1
Cu–O(1)	1.91(1)×4
Cu–O(2)	2.16(8)×1

The structure can be described as neutral $Bi_2Sr_2Ca_1Cu_2O_8$ slabs 13 Å thick, parallel to (001), with oxygen-deficient perovskite type. The slabs are weakly bonded together by long (3.0 Å) Bi–O bonds at $z=\frac{1}{4}$ and $\frac{3}{4}$. The arrangement at $z=\frac{1}{4}$ and $\frac{3}{4}$ can be viewed as a crystallographic shearing of the perovskite type.

The batch from which the crystal came was analyzed to an oxygen content of 8.13 per formula unit. It follows that other oxygen sites must be populated. The Wyckoff

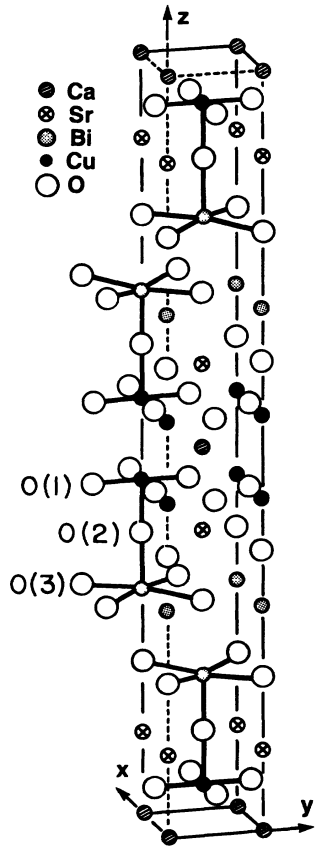

FIG. 2. Crystal substructure showing the unit cell of $Bi_2Sr_2Ca_1Cu_2O_8$. The O(4) is located directly below the O(1) midway between the Bi planes.

position 4*d* with coordinates $\frac{1}{2}, 0, \frac{1}{4}$ can geometrically accommodate as many as two extra oxygens per formula unit. Half-occupancy of this position would correspond to a total of 9 oxygens per formula unit, therefore to Cu(III). Accordingly, we introduced 0.065 oxygen atom O(4) on this site and we moved 0.13 bismuth toward this position at a distance of Bi–O(4) of 2.2 Å and used a population parameter of 0.87 for the remaining Bi site. This splitting of the Bi site alone lowered the weighted residual from 0.13 to 0.10 and this success indicates that this may well be the actual mechanism for the addition of oxygen.

Another interesting disorder also occurs at O(3) in the Bi plane. The stereochemical habit of Bi is to form two short bonds of approximately 2.2 Å with O, each corresponding to the exchange of nearly one valence unit, and a variable number of longer bonds. The apparent Bi–O(3) distance of 2.7 Å is only an average as indicated by the poor valence sum of O(3) and by subsidiary peaks around this atom on the difference-Fourier map. The correct local picture is that O(3) and Bi are displaced from the average position on the symmetry axis. No tetragonal symmetry can accommodate an ordered structure of this type with the present cell parameters: the Ca atom must be at a position of multiplicity 2 on the symmetry axis, and this fixes the origin; assuming a tetragonal space group, the site symmetry at Bi and O(3) is at least --2, forbidding their ordered displacement perpendicular to the *z* axis. Larger cells and possibly lower symmetry are required to accommodate the ordering of the short Bi–O(3) bonds. Electron diffraction performed on crystals from the same batch showed an incommensurate superstructure along [110], probably due to the ordering of the Bi–O(3) short bonds. It is quite likely that, depending on the oxygen content, several ordered superstructures and incommensurate modulations will be found. In these superstructures, the atoms equivalent to O(3) and Bi will be displaced by about 0.3–0.4 Å from their present average positions in an ordered fashion.

The present contribution is no more than a crude description of the substructure of $Bi_2Sr_2Ca_1Cu_2O_{8.13}$; nevertheless, it should be a useful starting point for further, more precise studies which will clarify, among other things, the mechanism for oxygen uptake.

OXYGEN CONTENT

The oxygen content in this compound has been determined by both its weight loss after reducing the material in hydrogen at temperatures up to 900 °C, and, more accurately, by chemical analysis. The thermogravimetric analysis (TGA) trace is shown in Fig. 3. From the weight loss after a reducing treatment we determine that the oxygen content is 8.25 ± 0.1 per unit formula 2,1.5,1.5,2 or 16.5 ± 0.2 per unit formula 4:3:3:4. The accuracy of this technique is frequently limited by the difficulty in determining, on the TGA curve, the temperature at which the reduction process is completed and the presence of a small amount of secondary oxide phases (e.g., CuO). A more accurate technique is a chemical analysis,[8] performed by dissolution of the compound in hydrochloric acid in the presence of an excess of Fe(II). Assuming the reaction Fe(II)+Cu(III) → Fe(III)+Cu(II), the remaining Fe(II) was back-titrated by Cr_2O_7 and this yields the amount of Cu(III) in the compound and thereby the oxygen content.

Although bismuth can usually exist in two oxidation states (III) and (V) within a perovskite structure (e.g., the Ba-Pb-Bi-O system), we considered that the Fi(II) oxidized was only that due to the Cu(III). An amount of 0.30 ± 0.05 Cu(III) and thereby an oxygen content of

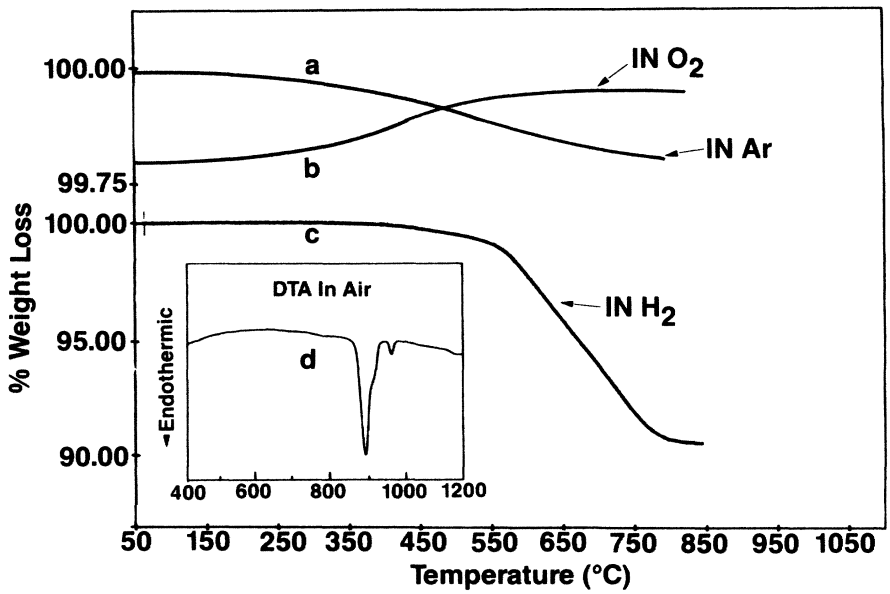

FIG. 3. Thermal analysis of the 4:3:3:4 phase. Thermogravimetric analysis shows weight loss by heating in argon (a) and weight gained by heating in oxygen (b). Weight loss due to reduction by heating in hydrogen is shown in curve (c). The inset (d) is a differential thermal analysis scan in air showing the melting transition. All scans were at 20 °C/min.

8.15 ± 0.02 per unit formula 2,1.5,1.5,2 was obtained by this analysis method. This value agrees well with the oxygen content determined by TGA. It is a common belief that an average copper valence greater than 2 is required to have superconductivity in the cuprate oxides; thus, with the small amount of Cu(III) determined by chemical analysis, the occurrence of Bi(V) in this compound is unlikely. Just as with the 90-K materials (e.g., $YBa_2Cu_3O_{7-y}$), the 4:3:3:4 phase is an oxygen-defect structure in which the copper has an average valence greater than 2 (about 2.15). Additional experiments (e.g., neutron diffraction) will be required to precisely determine the location of the oxygen defects.

TGA measurements were made to determine how the 4:3:3:4 compound is affected by different ambients. The material was treated as follows: The sample was first pretreated by heating under oxygen at 20 °C/min to 850 °C and cooled to remove adsorbed contaminants and make subsequent weight-loss measurements more reliable. Then, without exposing the sample to the laboratory ambient, it was heated under argon, subsequently cooled under argon, and then reheated under oxygen up to 850 °C with heating rates of 20 °C/min. Figure 3 shows the resulting TGA trace. Note that through this thermal cycle the oxygen loss and uptake is reversible but quite small (~0.1 oxygen atoms per unit formula) as compared to the 0.9 observed[9] for the $YBa_2Cu_3O_{7-y}$. Note that on heating in argon the compound loses up to 0.1 oxygen per unit formula [approximately the amount required to completely reduce Cu(III) to Cu(II) in this material] but still the material superconducts. We limit ourselves to a temperature of 850 °C because we observe that the compound melts at $885 °C \pm 10 °C$ in air as indicated (see Fig. 3, inset) by the endothermic peak located at 885 °C. We observe that the melting point in helium is 810 ± 10 °C. With respect to its oxygen affinity, this compound is more like the 40 K materials[10] ($La_{2-x}Sr_xCuO_{4-y}$) than the 90-K phase.[9] An x-ray powder pattern of the materials after being heated under argon revealed that the cell volume increased from 447 to about 450 Å^3, which may be ascribed to the conversion of Cu(III) to Cu(II). Plasma oxidation was performed in an attempt to increase the oxygen content beyond that obtained thermally and thereby change the material and its properties but no effect was observed. An attempt to increase the oxygen content in the 4:3:3:4 material by heating at 820 °C at 80 bars pressure in oxygen for 40 h resulted in a complete decomposition of the phase.

PHYSICAL PROPERTIES

Resistivity measurements as a function of temperature were made at constant current in a standard four-probe configuration. Silver ink contacts were used so that they could be removed with acetone prior to further processing of the sample. Figure 4(a) shows data for the highly oriented polycrystalline sample (denoted C1) and one sintered specimen (denoted P). For both samples, the resistivity decreases linearly from room temperature down to about 120 K. Below this temperature, note the deviation

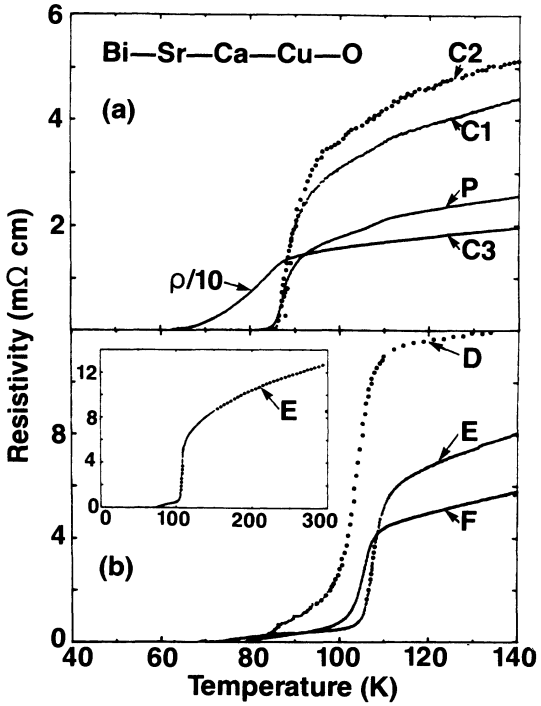

FIG. 4. Resistivity vs temperature from 40 up to 140 K. In (a) the polycrystalline 4:3:3:6 material (curve P) exhibits a T_c near 85 K. The multicrystalline composite as prepared, after oxygen annealing, and after argon annealing, as described in the text, are denoted C1, C2, and C3, respectively. In (b), curves D, E, and F are for materials annealed at 880 ± 5 °C for 48 h. The composition of the material for which curve D was measured is 4:3:3:6. Curves E and F are both for 4:3:3:4 composition material but annealed at slightly different temperatures as described in the text. The inset shows that the 110-K material deviates from linear resistivity below 200 K.

from linearity with a downward curvature to the superconducting onset near 90 K. The zero-resistance value is close to 85 K. For sample P, a very small resistivity drop can be detected at 115 K. This feature was not observed in the 4:3:3:6 composition when the ceramics were prepared by the method described above. It was, however, observed on samples deviating from this composition or processing procedure. The critical current for sample P, measured resistively, was 200 A/cm^2 at 4.2 K.

The changes in the temperature-dependent resistivity of this compound as function of processing in various ambients is also demonstrated in Fig. 4(a). The curves, obtained on the same as-grown multicrystalline composite, after 8 h oxygen anneal at 800 °C and after a 24 h vacuum anneal at 800 °C, are denoted C1, C2, and C3, respectively. Oxygen annealing did not significantly affect the resistivity, although T_c was enhanced by about 1 K ($R=0$ at 86 K). Plasma oxidation up to 60 h did not effect noticeable changes. These observations correlate well with the TGA measurements where only small changes in oxygen content were detected. The argon annealing increased the normal-state resistance by a factor of 4, and broadened and shifted T_c to lower temperature. A metal-

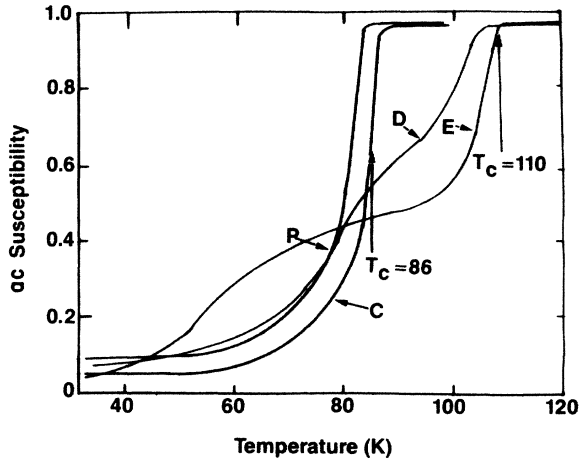

FIG. 5. ac susceptibility vs temperature from 30 to 120 K for several compositions in the Bi-Sr-Ca-Cu-O system and as a function of thermal processing. Sample designations are described in the text.

liclike resistivity (positive temperature coefficient) above T_c to room temperature was measured.

The superconducting transition temperatures were also determined by an ac mutual inductance apparatus and the traces of the superconducting transition are reported for the samples C and P in Fig. 5. Both ac susceptibility and resistivity measurements give similar values for the onset of the superconducting transitions (the thermometers used in both measurements are calibrated to 0.2 K) but the ac transitions are broader.

The experiments described thus far indicate that the material is a superconductor but do not prove bulk superconductivity. Thus, we measured the screening and exclusion of magnetic flux with a superconducting quantum interference device (SQUID) magnetometer. The results obtained for powdered sample P after cooling in zero field and warming it in a field of 10 G are shown in Fig. 6. The onset of superconductivity occurs at a temperature similar to that observed by both resistivity and ac measurements. From the magnetization, weight, and volume of the sample we calculate a Meissner signal which is 54% of that expected and therefore evidence for bulk superconductivity in this compound. This value is overestimated because the demagnetization factor n was not taken into account. Complete Meissner susceptibility should lead to $M=-1/(1-n)(1/4\pi)$ times the applied field whereas we have taken $M=-(1/4\pi)H_{\text{applied}}$ for our calculation. The magnetic susceptibility above T_c is shown in Fig. 6 (inset). The data do not follow a Curie-Weiss law, in contrast to the 90-K phase previously reported, but instead show a slight negative curvature with decreasing temperature. From the value of the susceptibility (χ_0), and after correction for core diamagnetism, we obtain a value of $\chi_p=10^{-4}$ emu/mol of Cu. This value is about two times smaller than that reported,[9] per copper atom, for the Y-Ba-Cu-O phase. However, χ_p can also be affected by electron-electron effects and these interactions could be different between two materials. Thus it would be of interest to measure the specific heat at low temperatures as an additional characterization of the difference between the two materials. It may be coincidental, but we also note that the concentration of Cu(III) we determined by chemical analysis and TGA for the 4:3:3:4 material is also a factor of 2 lower than that obtained for the $YBa_2Cu_3O_{7-y}$ phase.

SUPERCONDUCTIVITY AT 110 K

Maeda *et al.* also reported that annealing the 1:1:1:2 composition at 880 °C was necessary to obtain the 110-K superconducting transition. Accordingly, we investigated the effect of thermal processing on the properties of the

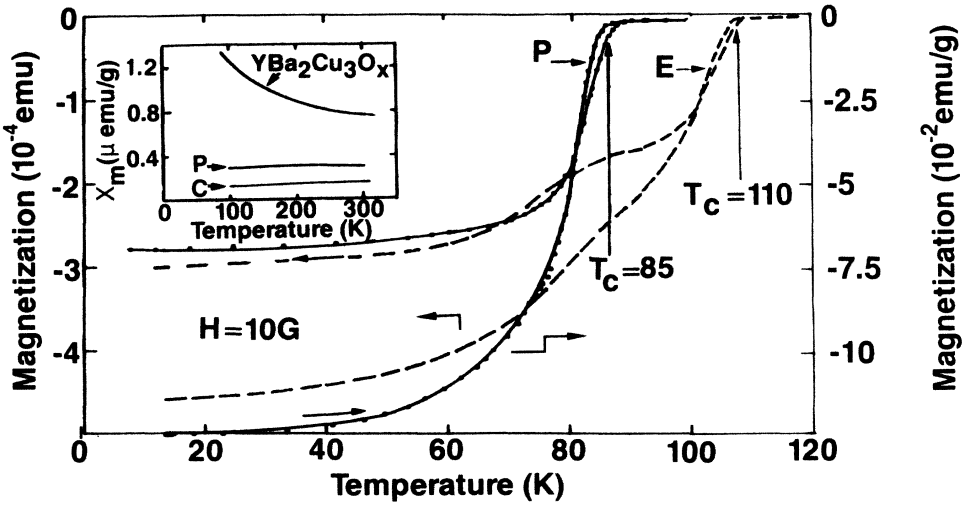

FIG. 6. Magnetization vs temperature for samples E (dashed line) and P (solid line). The upper curves are for cooling in a field of 10 G (Meissner) and the lower curves are for warming in a field of 10 G (shielding). The inset shows the susceptibility over a broad temperature range in comparison to $YBa_2Cu_3O_7$. The weight of sample E was 4 mg.

4:3:3:4 compound. We observe that heat treating this compound very close to but not above its melting point generates a material with a T_c of 110 K. Thermal treatments 20 °C above the melting point degrade the superconducting properties of the 4:3:3:4 phase as well as its structure. Heat treatments up to 850 °C produce no detectable changes in either the superconducting properties (T_c = 85 K) or the x-ray powder diffraction pattern. However, heat treating at 870 °C for 24 h produces a material in which 20% of the diamagnetic shift of the ac susceptibility shows a T_c of 110 K and the balance a T_c of 85 K. But still the x-ray powder-diffraction pattern does not evidence a noticeable change. After heat treating at a higher temperature (880 °C) for a longer time, 50% of the ac susceptibility shows a T_c of 110 K and the balance a T_c of 85 K, as shown in Fig. 5, curves D and E. Among the samples investigated, we find that the amplitude of the ac signal corresponding to the 110-K T_c was largest for the samples that showed some decomposition (a bronze color on the back of the pellet, in contact with the alumina crucible). Rutherford backscattering and scanning electron microscopy of the backside of the pellet show an excess of calcium and copper. Thus the bulk materials become deficient in calcium at high temperature, leading to the possibility of a phase rich in strontium. The x-ray powder pattern of specimens E and F, which contain large amounts of the 110-K phase, is different than that of Fig. 1 due to the presence of secondary phases. But still, the 4:3:3:4 predominates. Clearly, the long times at high temperatures, necessary to produce material with the 110-K T_c, indicate a transformation or atomic motion having slow kinetics.

The resistivity versus temperature for three materials exhibiting strong superconducting transitions near 110 K are reproduced in Fig. 4(b). The composition of the materials were 4:3:3:6 for curve D and 4:3:3:4 for curves E and F. The inset in Fig. 4(b) shows the resistivity of sample E from 0 to 300 K. Note that the 110-K material deviates from a linear resistivity below 200 K, exhibiting a negative curvature down to T_c. This is in contrast to $YBa_2Cu_3O_{7-y}$ which exhibits a linear resistivity versus temperature from room temperature down to a few degrees above the superconducting transition and the 85 K Bi-Sr-Ca-Cu-O phase which exhibits a linear behavior down to about 125 K. It is interesting to note that curves E and F were measured on samples not only having the same composition and prepared at the same time, but reannealed together in the same furnace. Temperature gradients in the furnace caused sample E to be heated about 5 °C more than sample F, which caused a slight decomposition in sample E as was observed by a black residue on the alumina crucible. Note that sample E exhibits a higher T_c by 3 K. These curves demonstrate just how sensitive the 110-K phase is to processing. It is important to note that, although these materials exhibit a sharp resistance drop near 110 K, zero resistance is not observed above 80 K. This long resistivity foot present in all the samples exhibiting the 110-K transition is puzzling and raises questions as to the origin of the superconductivity at 110 K. To examine this point, we measured the Meissner effect for sample E (which shows the highest T_c resistivity and the maximum diamagnetic ac signal). The trace of the Meissner and shielding effects are shown in Fig. 6. We observe a total Meissner effect of 50% with 26% and 24% corresponding to the 110 and 85-K transitions, respectively. This result unambiguously confirms the existence of bulk superconductivity at 110 K in the Bi-Sr-Ca-Cu-O system. However, we have not as yet been able to obtain a single-phase 110-K material.

DISCUSSION

We have shown that a phase of composition 4:3:3:4 is responsible for superconductivity at 85 K in the Bi-Sr-Ca-Cu-O system. Structural studies have shown that this phase has features similar to the well-known superconducting oxygen-defect perovskites La_2CuO_4 and $YBa_2Cu_3O_{7-y}$. This structure does not contain Cu—O chains, but we believe that the adjacent bismuth may play an important role. The most striking common feature to all these cuprate-based superconductors is a valence of Cu greater than 2.

Single-crystal diffraction studies lead to the formula 4:4:2:4 for the superconducting phase. However, attempts to prepare a single-phase material from this composition were unsuccessful. One explanation is that from the range of mutual solubility we observed ceramic compacts may consist of crystals with a varying composition. Thus, since the largest crystals in the compact were selected for the single-crystal structure studies, it may be that the 4:4:2:4 composition reflects a slightly higher growth rate.

Let us now consider the 110-K material. We have powder specimens that show a 50% total Meissner effect, half of which is due to the 110-K transition. The powder x-ray diffraction patterns (of the 110-K material) show the main peaks corresponding to the 4:3:3:4 phase with several extra peaks most likely due to secondary phases because of partial decomposition of the material. A broad background of diffuse scattering (centered at approximately 30° with $\Delta 2\theta$ at half maximum of approximately 7°), possibly due to an amorphous phase, was observed.

Since the 110-K phase forms mainly during decomposition, it may be that each particle is surrounded by a lower T_c or nonsuperconducting material. The similarity in Meissner and shielding effects and the existence of the resistive foot are consistent with this statement. This is also consistent with the observation of extra peaks in the powder x-ray diffraction, which would preferentially sample the outside of the grains.

Interestingly, a fitting of the Bragg peaks corresponding to the 4:3:3:4 phase in the powder-diffraction pattern of the material containing the 110-K phase gave the following lattice parameters; $a = 3.82$ and $c = 30.7$ Å. Within experimental error, these values are identical to those obtained for the 85-K phase. At this point there are two possibilities. First, the Bragg peaks corresponding to this phase are mixed with impurity phases so that we cannot determine which lines correspond to the 110-K compound. Second, the 110-K phase has identical structure (as determined by powder x-ray diffraction) to the 85-K phase. Structural changes that may accompany the increase in

T_c are subtle enough so as to require a more detailed characterization, which we have undertaken. The types of changes we envisage, which would have low kinetics and yet not produce marked structural rearrangements, include (1) some loss of one (or more) of the cation components creating cation vacancies; (2) a change in the bismuth valence and oxygen coordination [bismuth introduces a new factor in these materials in that in the +3 valence state it is large enough to occupy the large cation sites in the perovskite structure whereas in its other +5 valence state it is small enough to occupy the small cation sites (i.e., substitute for Cu)]; and finally (3) an order-disorder or ordering of some of the cations (e.g., Sr, Ca) where we distinguish between a process which is ordered at low temperatures and disordered at high temperatures due to entropic considerations and a process which is disordered as prepared but wants to order due to energy consideration and requires high temperatures and long times because atomic mobility is small. Further work is required to understand the differences between the 85 and 110-K states.

ACKNOWLEDGMENTS

We thank C. C. Chang, L. A. Farrow, W. L. Feldman, B. Meagher, P. F. Miceli, W. L. Quinn, J. M. Rowell, E. A. Vogel, J. H. Wernick, and B. J. Wilkins for assistance.

[1]J. G. Bednorz and K. A. Müller, Z. Phys. B **64**, 189 (1986).

[2]M. K. Wu, J. R. Ashburn, C. J. Torng, P. H. Hor, R. L. Meng, L. Gao, Z. J. Huang, Y. Q. Wang, and C. W. Chu, Phys. Rev. Lett. **58**, 908 (1987).

[3]C. Michel, M. Hervieu, M. M. Borel, A. Grandin, F. Deslandes, J. Provost, and B. Raveau, Z. Phys. B **68**, 421 (1987).

[4]J. Akimitsu, A. Yamazaki, H. Sawa, and H. Fujiki, Jpn. J. Appl. Phys. **26**, L2080 (1987).

[5]H. Maeda, Y. Tanaka, M. Fukutomi, and T. Asano, Jpn. J. Appl. Phys. Lett. **4**, L209 (1988).

[6]C. W. Chu, cited in *The New York Times,* 28 January 1987, p. C2.

[7]Upon completion of this work, we received a copy of unpublished work by Hazen *et al.*, discussing superconductivity and phase identification in the Bi-Ca-Sr-Cu-O system.

[8]B. Raveau (private communication).

[9]J. M. Tarascon, W. R. McKinnon, L. H. Greene, G. W. Hull, and E. M. Vogel, Phys. Rev. B **36**, 226 (1987).

[10]J. M. Tarascon, L. H. Greene, W. R. McKinnon, G. W. Hull, and T. H. Geballe, Science **235**, 1373 (1987).

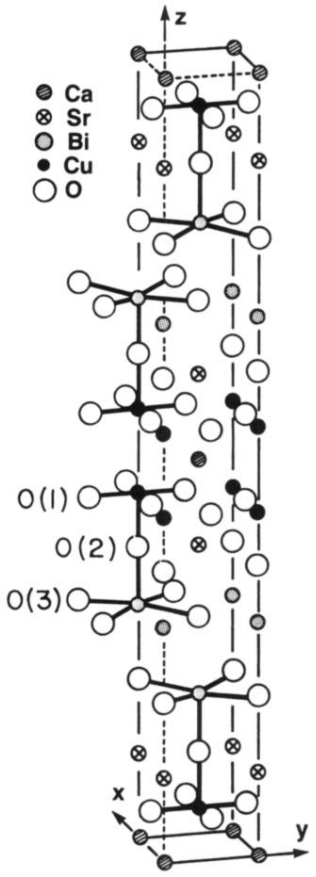

FIG. 2. Crystal substructure showing the unit cell of $Bi_2Sr_2Ca_1Cu_2O_8$. The O(4) is located directly below the O(1) midway between the Bi planes.